Table II. Results of Energy Decomposition for $Ni(O_2)(N_2)$ with End-On and Side-On Geometries (kcal/mol)

	end-on	side-on		end-on	side-on
ES	−56.0	−41.7	BCTPLX	−26.5	−28.3
EX	72.1	73.4	MIX	0.6	−8.2
FCTPLX	−24.5	−14.9	ΔE_T	−34.3	−19.7

2 is very easy. The rotational barrier from side-on to end-on coordination of the N_2 ligand is small while the energy required for the opposite direction is large. Therefore, even if the complex with dioxygen and dinitrogen ligands coordinating in the side-on manner forms, it will rapidly return to the most stable structure that has the end-on dinitrogen and side-on dioxygen ligands. Ozin et al. could not find the IR spectra indicating the N_2 side-on geometry. This experimental evidence is consistent with the present calculation results.

Nature of Bonding between Ni and N Atoms. As mentioned above, the complex with the end-on N_2 ligand is more stable than that with the side-on one. This result is consistent with the trend observed in many dinitrogen complexes. Therefore, it is very interesting to discuss this property in these geometrical isomers. To analyze the bonding nature of the Ni–N bond, the interaction energy[14] between $Ni(O_2)$ and N_2 fragments, ΔE_T, is decomposed to several types of energies such as ΔE_{ES}, ΔE_{EX}, ΔE_{FCTPLX}, ΔE_{BCTPLX}, and ΔE_{MIX} by use of the energy decomposition technique of Kitaura and Morokuma.[6] The first two terms represent energies of electrostatic (ES) interaction and exchange (EX) repulsion. ΔE_{FCTPLX} and ΔE_{BCTPLX} are coupling terms of charge-transfer (CT) and polarization (PL) interactions.[15] They are defined as donative and back-donative interactions, respectively. The last term is a coupling energy of all above components. Results are listed in Table II. The interaction energies for end-on and side-on complexes are calculated to be −34.3 and −19.7 kcal/mol, respectively. The sums of total energies of the two fragments are −1760.7656 and 1760.7634 au, respectively. As the difference of these energies is very small, the relative stability of the geometrical isomers is determined by the magnitude of the interaction energies. The absolute value of ΔE_{ES} of **1** is larger by 14.3 kcal/mol than that of **2**. Moreover, that of ΔE_{FCTPLX}, which is the contribution of the σ donation, is large in **1** in comparison with that in **2**. Therefore, the relative values of these contributions indicate that the end-on coordination is preferred to the side-on structure.

Acknowledgment. Permission to use the FACOM M-200 Computer at the Data Processing Center of Kyoto University is gratefully acknowledged. The authors also thank the Computer Center, Institute for Molecular Science, for the use of the HITAC M-200H Computer. The work was carried out by a Grant-in-Aid from the Ministry of Education of Japan.

Registry No. **1**, 41772-91-2.

(14) The interaction energy is defined as the difference between the total energy of $Ni(O_2)(N_2)$ and the sum of those for the two fragments $Ni(O_2)$ and N_2.

(15) Kitaura, K.; Sakaki, S.; Morokuma, K. *Inorg. Chem.* **1981**, *20*, 2292.

Contribution from the Research School of Chemistry, Australian National University, Canberra, Australia 2600

Inequivalent Clusters and Energy Transfer in Trinuclear Chromium(III) Acetate

LUCJAN DUBICKI,* JAMES FERGUSON,* and BRYCE WILLIAMSON

Received March 2, 1983

Below 211 K the structure of hydrated chromium acetate, $[Cr_3O(CH_3CO_2)_6(H_2O)_3]Cl\cdot 6H_2O$, consists of equal numbers of two inequivalent trimers, a and b. Dehydration produces domains of an anhydrous phase characterized by species c and d, each consisting of a family of inhomogeneous members. Selectively excited emission and excitation spectra, as well as fluorescence-lifetime measurements, show evidence for energy transfer d → c and a → b. The mechanism is identified as a pure electronic resonant energy transfer $(^7/_2{}^*)_a(^5/_2)_b \rightsquigarrow (^7/_2)_a(^7/_2{}^*)_b$ ($\Delta S_a = 0$; $\Delta S_b = +1$). Energy transfer between higher lying excited states is quenched by a faster intracluster radiationless relaxation.

1. Introduction

The electronic structure, in particular the order of the ground electronic levels, of basic chromium(III) acetate, $[Cr_3O(CH_3CO_2)_6(H_2O)_3]Cl\cdot 6H_2O$, has stimulated considerable interest.[1-6] It is now established that at low temperatures the structure of the hydrated chloride salt consists of equal numbers of two inequivalent trimeric clusters, labeled a and b.[3,6] Recently, Morita and Kato[4] have reported new emission lines, here labeled c and d, in addition to those associated with clusters a and b. Their assignment of c and d to stressed clusters was not supported by our preliminary spectroscopic measurements, and the first objective of the present work was the characterization of the origin of the lower lying energy levels of species c and d.

From studies of excitation spectra we obtained evidence for energy transfer from a to b and from c to d. Energy transfer between the lowest lying excited states $S_a{}^* = {}^7/_2$ and $S_b{}^* = {}^7/_2$ was also noted by Morita and Kato.[4] Independently, Schenk and Guedel[6] examined this problem in more detail and proposed a phonon-assisted energy-transfer mechanism involving intercluster exchange. Estimates of the latter were low ($J_{ab} < 0.1$ cm^{-1}), which led to criticism of a recent reanalysis of the thermal and magnetic properties of the hydrated chloride salt.[5] In this connection it is important to emphasize that spectroscopic techniques are far more sensitive than "direct" X-ray structure methods for the detection of inequivalent molecules. For example, the X-ray analysis of $[(NH_3)_5Cr(OH)Cr(NH_3)_5]Cl_5\cdot H_2O$ showed only one dimeric species,[7] whereas spectroscopic measurements gave clear

(1) Sorai, M.; Tachiki, M.; Suga, H.; Seki, S. *J. Phys. Soc. Jpn.* **1971**, *30*, 750 and references therein.
(2) Dubicki, L.; Day, P. *Inorg. Chem.* **1972**, *11*, 1868.
(3) Ferguson, J.; Guedel, H. U. *Chem. Phys. Lett.* **1972**, *17*, 547.
(4) Morita, M.; Kato, Y. *J. Quant. Chem.* **1980**, *18*, 625.
(5) Wrobleski, J. T.; Dziobkowski, C. T.; Brown, D. B. *Inorg. Chem.* **1981**, *20*, 684.
(6) Schenk, K. J.; Guedel, H. U. *Inorg. Chem.* **1982**, *21*, 2253.
(7) Veal, J. T.; Jeter, D. Y.; Hempel, J. C.; Eckberg, R. P.; Hatfield, W. E.; Hodgson, D. J. *Inorg. Chem.* **1973**, *12*, 2928.

0020-1669/83/1322-3220$01.50/0

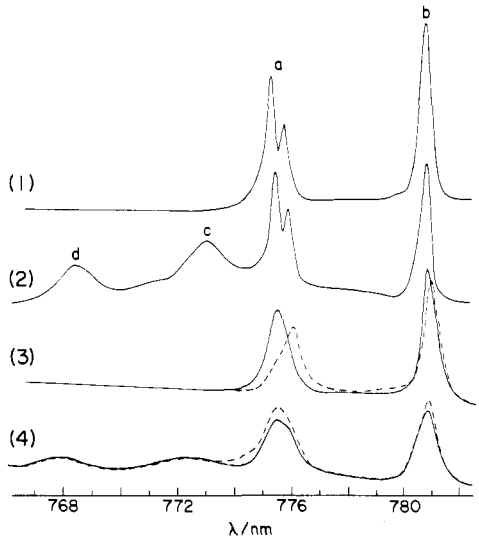

Figure 1. (1) Unpolarized emission of hydrated chloride crystal at 6 K, excitation at 650 nm. (2) Unpolarized emission of dehydrated crystal at 6 K. (3) Polarized absorption spectra of hydrated crystal at 60 K: full line, $E \parallel B$; dashed line, $E \parallel A$ (where A and B are the extinction directions defined in ref 2). (4) Polarized absorption spectra of dehydrated crystal at 60 K.

evidence of equal numbers of two inequivalent dimers.[8] Subsequently a redetermination of the crystal structure of the monohydrate indicates that a series of very weak diffraction spots, previously attributed to twinning, are real. The true cell is doubled along the c axis, implying equal numbers of two inequivalent dimers. A partial refinement of the structure reveals no significant structural difference between the two species.[8,9] A similar example is found in the corresponding trihydrate complex. Here, the crystal structure determination shows only one dimer,[10] whereas selectively excited emission and excitation spectra show the presence, in smaller concentration, of a second dimer.[11]

The energy-transfer mechanism proposed by Schenk and Guedel[6] is essentially the process $(^7/_2{}^*)_a(^7/_2)_b \rightsquigarrow (^7/_2)_a(^7/_2{}^*)_b + h\bar{c}\bar{\nu}$, where $\bar{\nu} \approx 80$ cm^{-1}. This assignment does not explain the absence of back-transfer between 30 and 60 K. The predicted temperature dependence of the rate constant of the energy transfer, k_e, on the Boltzmann population of the ground-state level $S_b = {}^7/_2(P_{(7/2)_b})$ is not consistent with our temperature dependence of the excitation spectra. Accordingly, the second objective of the present work was a more detailed analysis of the mechanism of energy transfer.

2. Experimental Section

2.1. Preparation of Crystals. The acetate salt of basic chromium(III) acetate was prepared by the method of Weinland.[12] Dissolution in dilute HCl and slow evaporation gave high-quality rectangular (110) and pseudohexagonal (001) plates of the hydrated chloride salt. The partly dehydrated crystals were produced by slowly cooling the hydrated crystals in a stream of dry He gas. Rapid cooling produced only minute concentrations of the anhydrous phase. Dehydration proceeds rapidly on the surface and depolarizes the absorption spectrum. The process was monitored by measurement of the emission spectrum, which was characterized by the appearance of the new bands c and d (see Figure 1). Dehydration is partly reversible, and exposure of dehydrated crystals to a moist atmosphere for several hours increased the emission intensity of a and b at the expense of lines c and d. Morita and Kato[4] suggested that c and d might be due to stressed crystals. This explanation was tested by the application of uniaxial stress, either parallel or perpendicular to the c axis of the hydrated crystals, protected by transparent coatings of rubber cement. Even for applied pressures of about 100 kPa, at which the crystals shattered, no emission from c or d was observed. It is clear that c and d must represent emission lines associated with an anhydrous phase.

The hydrated chloride salt has a phase transition at 211 K.[1] Recent X-ray diffraction studies[6] at 190 K show that the structure changes from $P2_12_12$ ($Z = 4$) at room temperature to $P2_12_12_1$ ($Z = 8$) and the unit cell is doubled along the c direction, thereby confirming an earlier suggestion[1] that equal numbers of a and b clusters are present below 211 K. The full crystal structure was not determined. From the structural data at 295 K,[13] we calculate for the low-temperature space group that a given cluster will have five first-nearest-neighbors (1nn) of opposite type (a–b) with intercluster separations (distances between central oxygen atoms) 8.06 and 9.14 (2) Å. The other two are either a or b with separations of 8.38 Å. For convenience we assume five (a–b) 1nn.

2.2. Spectroscopy. The emission and excitation spectra were excited by a 150-W Xe lamp or a Molectron DL 200 dye laser pumped with a Molectron UV1000 nitrogen laser. For the former a Spex 1402 spectrometer was used to obtain the excitation wavelength. The emission was dispersed by a Spex 1704 monochromator and detected by a cooled RCA 31034 photomultiplier and either a Keithley 417 picoammeter or a PAR 162 Boxcar averager. Most samples were cooled in a helium gas flow tube. In other cases, excited by the dye laser, they were cooled in a Janis DT 10 cryostat. Temperatures were monitored by either a gold–chromel thermocouple or a carbon resistor. The dye laser was used for decay time measurement as well as for time resolved work. Absorption spectra were recorded by a Cary 17 spectrophotometer using a Hamamatsu 928 photomultiplier. Stress experients were made by using a hydraulic stress cell fabricated in this school. For measurements of excitation spectra above 750 nm (a and b), Xe lamp excitation was used, but for c and d, lying to higher energy, the dye laser had sufficient intensity to use as an excitation source and consequently higher resolution was achieved.

3. Results

3.1. Low-Energy Levels of Inequivalent Clusters. Selectively excited emission and excitation spectra were used to resolve and characterize the inequivalent species a, b, c, and d. Figure 2 shows the excitation spectra of species a and b under Xe lamp excitation (section 2.2). The spectra of c and d were poorly resolved, and higher resolution was obtained with dye laser excitation (Figure 3).

The analysis of the spectra of species a and b, given in Figure 2, is similar to an earlier analysis.[3] Species a and b evidently remained fully hydrated in the partly dehydrated crystal. The excitation spectra of c and d differ from a and b in two respects. Both c and d consist of two groups of subspecies c_1, c_2, d_1, and d_2 (Figure 3). Furthermore, each subspecies consists of a family of inhomogeneous members, and a good example of the resultant inhomogeneous broadening is given in Figure 4. Here the emission spectra of c_1 are partially resolved and similar, but less well-resolved, emission spectra are associated with c_2, d_1, and d_2. The severe inhomogeneous broadening makes it impossible to determine whether c and d clusters are distorted from the idealized D_{3h} cluster geometry, and only the average ground-state exchange parameters were obtained, viz., $J_0 \simeq +20$ cm^{-1} for c_1, c_2 and $J_0 \simeq +22.5$ cm^{-1} for d_1, d_2 with

$$\mathcal{H}_{ex} = +J_0 \sum_{i<j} \mathbf{S}_i \cdot \mathbf{S}_j$$

The experimentally determined ground and lower lying excited states are given in Figure 5.

The low-lying excited states in all species have the same pattern and relative energies. This fact and the close similarity of the J_0 values indicate that each species has the same chromophore $[Cr_3O(CH_3COO)_6(H_2O)_3]^+$, so that the inequivalency arises from different outer-sphere structures, which involve loosely bound H_2O molecules and fractionally occupied Cl^- sites.[13]

(8) Ferguson, J.; Guedel, H. U.; Puza, M. *Aust. J. Chem.* **1973**, *26*, 513.
(9) McLaughlin, G.; Robertson, G. B., unpublished work.
(10) Engel, P.; Guedel, H. U. *Inorg. Chem.* **1977**, *16*, 1589.
(11) Dubicki, L., to be submitted for publication.
(12) Weinland, R. *Ber. Dtsch. Chem. Ges.* **1908**, *41*, 3236.
(13) Chang, S. C.; Jeffrey, G. A. *Acta Crystallogr., Sect. B* **1970**, *B26*, 673.

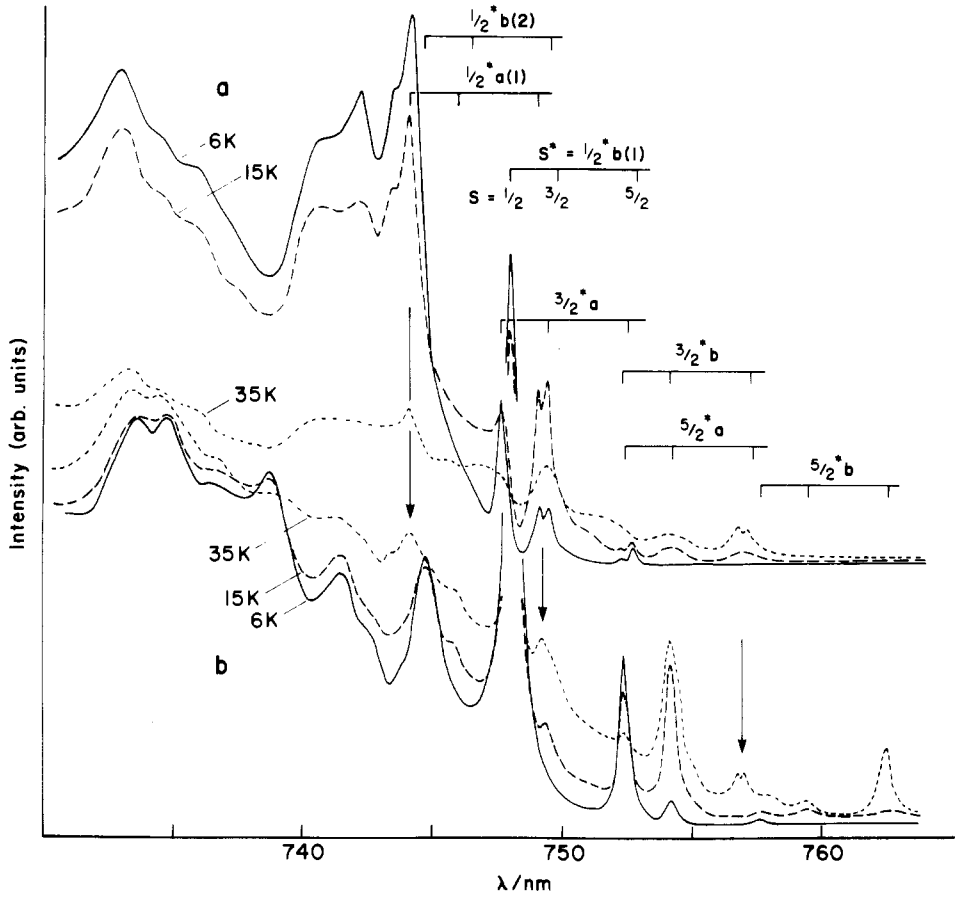

Figure 2. Excitation spectra of clusters a and b with Xe lamp excitation. Similar spectra were obtained for both hydrated and dehydrated crystals. The assignments (S* = excited state; S = ground state) are straightforward. Specific cases of energy transfer a–b are indicated by arrows.

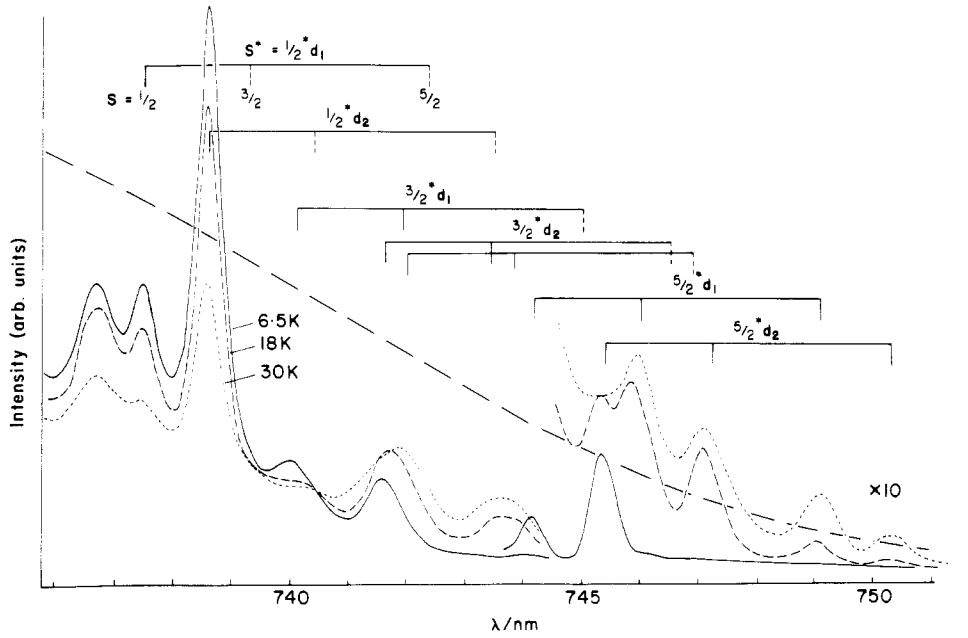

Figure 3. Excitation spectra of cluster d with dye laser excitation. The variation in the laser power is indicated by the dashed line. Similar spectra were obtained for cluster c.

3.2. Intercluster Energy Transfer. The possibility of energy transfer from a to b was first suggested by Morita and Kato.[4] The temperature dependence of the emission intensities was examined in more detail by Schenk and Guedel,[6] who proposed a phonon-assisted energy-transfer mechanism: $(^7/_2{}^*)_a(^7/_2)_b \rightsquigarrow (^7/_2)_a(^7/_2{}^*)_b + h\bar{c}\bar{\nu}$, where the electronic energy gap (Figure 5) is bridged by a phonon with $\bar{\nu} \simeq 80$ cm^{-1}. Similar experiments on the dehydrated crystals (Figure 6) indicate both a to b and d to c energy transfers. Additional evidence for d to c transfer is also obtained from the dye laser excitation of d. Because of the large inhomogeneous broadening, the d to c transfer was not examined further. Instead, we analyzed more carefully the temperature dependence of the decay curves for the a and b species in fully hydrated crystals.

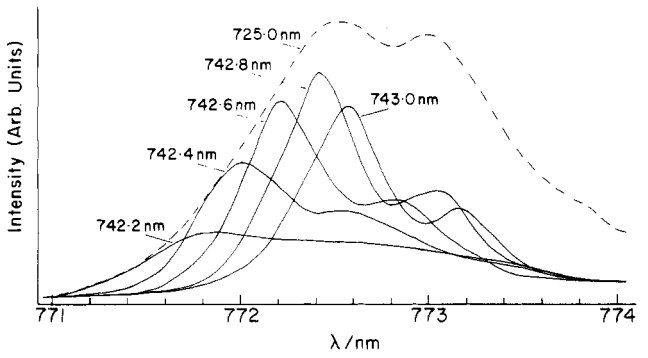

Figure 4. Fluorescence line-narrowed spectra of cluster c for various dye laser excitation wavelengths of the $(^1/_2{}^*)_{c_1}$ state (742.2–743.0 nm). Excitation at 725.0 nm (dashed line) gives inhomogeneously broadened emission. Similar examples of fluorescence line narrowing were obtained for $(^1/_2{}^*)_{d_1}$, $(^1/_2{}^*)_{d_2}$, and $(^1/_2{}^*)_{c_2}$ states, but the emission spectra were not as well resolved as for $(^1/_2{}^*)_{c_1}$.

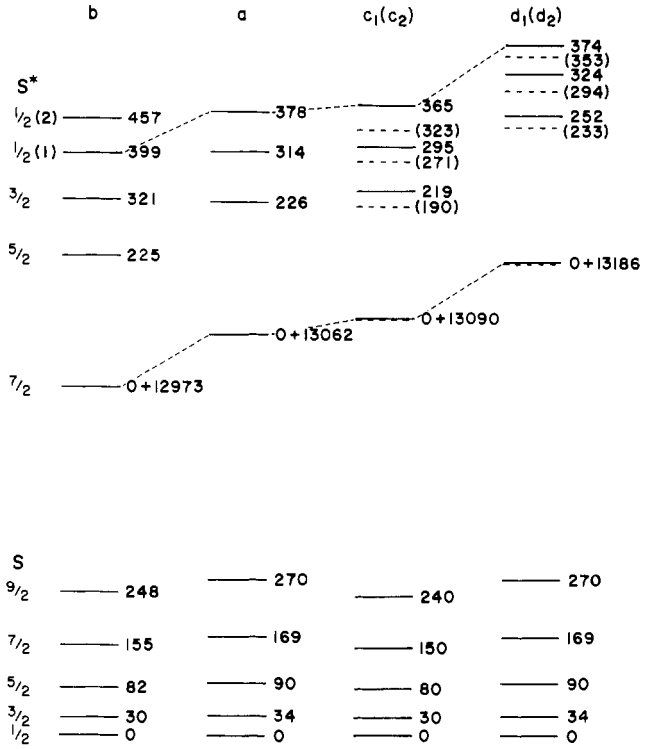

Figure 5. Ground and lower lying excited states for clusters a, b, c, and d. The low-symmetry splittings of the ground levels for a have been averaged.

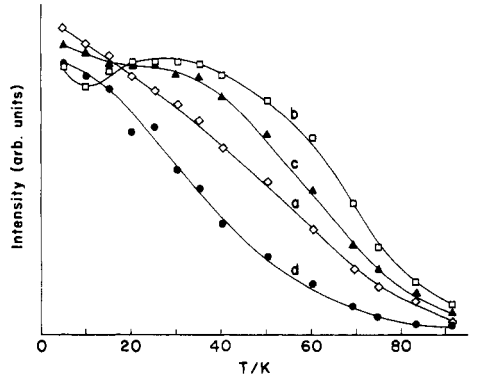

Figure 6. Temperature dependence of the emission intensities from clusters a, b, c, and d (excitation wavelength 450 nm).

Pulsed excitation at 450 nm, using the dye laser, leads to a nearly equal population of the excited levels $S_a{}^* = {}^7/_2$ and $S_b{}^* = {}^7/_2$, as indicated by the relative emission intensities. The

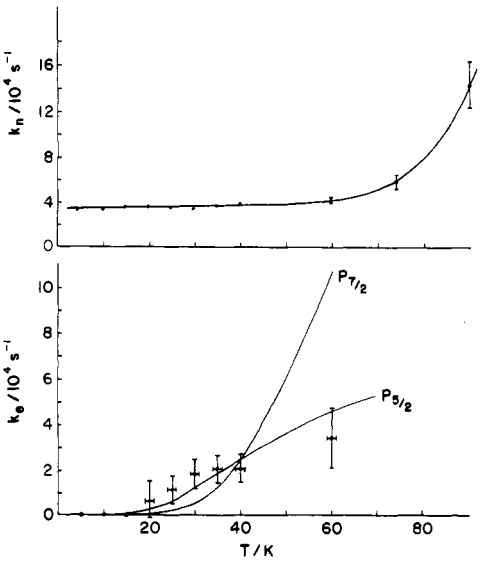

Figure 7. Temperature dependence of the radiationless (k_n) and energy transfer (k_e) rates. The latter is compared to the Boltzmann populations of the ground $^7/_2$ and $^5/_2$ levels ($J_0 = 20.5\ cm^{-1}$) by normalizing the populations at 40 K.

oscillator strengths of the transitions $^7/_2 \rightarrow {}^7/_2{}^*$ are $\sim 24 \times 10^{-8}$ (per mole of cluster and corrected for $P_{7/2}$) and give a very small value for the radiative rate, $k_{r(7/2^* \rightarrow 7/2)} = 27\ s^{-1}$. The corresponding radiative lifetime, $\tau_r \simeq 0.038\ s^{-1}$ is much longer than the measured decay times at 5 K, viz., $\tau_a \simeq 31 \times 10^6$ s and $\tau_b \simeq 30 \times 10^{-6}$ s. The temperature dependence of the decay rates can therefore be analyzed on the basis of the rate equations

$$d[N_{7/2^*}]_a/dt = -(k_n + k_e)[N_{7/2^*}]_a \quad (1)$$

$$d[N_{7/2^*}]_b/dt = k_e[N_{7/2^*}]_a - k_n[N_{7/2^*}]_b \quad (2)$$

where k_n is the radiationless decay rate for $S^* = {}^7/_2$, $k_{na} \simeq k_{nb}$, k_e is the rate of energy transfer from a to b, and N_i is the population of level i. In agreement with this model, the decay times for species a could be fitted accurately with a single-exponential function while the b decay times required a double-exponential fit. The analysis of the experimental data is given in Figure 7.

The radiationless rate k_n is constant ($4 \times 10^4\ s^{-1}$) over the range 10–60 K and increases sharply above 60 K. It was not possible to examine the mechanism for radiationless deactivation in detail because the emission line becomes very weak above 100 K. The temperature dependence of k_e follows the Boltzmann distribution for $S = {}^5/_2$ with $J_0 = 20.5\ cm^{-1}$. If we put $k_e = k_e{}^\circ P_{5/2}$, then $k_e{}^\circ \simeq 2 \times 10^5\ s^{-1}$. This result suggests that the energy transfer is a pure electronic resonance process, $(^7/_2{}^*)_a(^5/_2)_b \rightsquigarrow (^7/_2)_a(^7/_2{}^*)_b$ ($\Delta S_a = 0$; $\Delta S_b = +1$). The energy gap $E_{(7/2^*)a} - E_{(7/2^*)b} - E_{(7/2)a} = -80\ cm^{-1}$ is bridged almost exactly by excitation of the ground $(^5/_2)_b$ level (see Figure 5). This mechanism also explains the absence of any back-transfer at about 40 K (Figure 2), since this will depend on $(P_{7/2})_a$.

4. Discussion

The rate constant for resonant energy transfer is given by

$$k_e(a \rightarrow b) = 4\pi^2 c|\langle a^*b|\mathcal{H}|ab^*\rangle|^2 \int g_a g_b\, d\bar{\nu} \quad (3)$$

where g_a and g_b are the normalized donor emission and acceptor absorption line shape functions, respectively. We can estimate the value of the matrix element using $k_e{}^\circ \simeq 2 \times 10^5\ s^{-1}$ and assuming that only the 5 1nn b clusters surrounding each a cluster (section 2.1) are important. In addition, we need to know the spectral overlap integral $\Omega = \int g_a g_b\, d\bar{\nu}$. Unfor-

tunately, g_b, which corresponds to the line shape for the absorption $(^5/_2)_b \rightarrow (^7/_2{}^*)_b$ is masked by the more intense $(^7/_2)_a \rightarrow (^7/_2{}^*)_a$ process. We know that $\Delta S = +1$ transitions (Figure 2) have an oscillator strength $f_{\Delta S=+1} = {}^1/_{10} f_{\Delta S=0} \simeq 24 \times 10^{-9}$, and since all the well-resolved bands in Figures 1 and 2 have Gaussian line shapes with bandwidths (fwhh) ranging from $\bar{\nu}_{1/2} \simeq 6$ cm^{-1} for $(^1/_2) \rightarrow (^1/_2{}^*)$ to ~ 9 cm^{-1} for $(^7/_2) \rightarrow (^7/_2{}^*)$, we can calculate Ω assuming Gaussian line shapes. This procedure, however, is not valid since the moderately large bandwidths in absorption are undoubtedly due to inhomogeneous broadening. In our neat solid-state problem, there is a strong correlation between the structure of a and the structure of the 1nn b clusters. The correct bandwidth to use in the calculation of Ω will tend toward the homogeneous width appropriate for a pair of a and b clusters.[14] This value of $\bar{\nu}_{1/2}$ should be significantly smaller, perhaps <1 cm^{-1}, and the line shape may be Lorentzian. Unfortunately, we were unable to make a line shape study of the a and b clusters using the dye laser so we have no idea of the values of the homogeneous bandwidths.

On the assumption of a Lorentzian line shape with $\bar{\nu}_{1/2} \simeq 1$ cm^{-1}, we calculate for two Lorentzian lines with the same widths and peak maxima displaced by δ (in cm^{-1})

$$\Omega_L = 1/[\pi\bar{\nu}_{1/2}(1 + (\delta/\bar{\nu}_{1/2})^2)] \quad (4)$$

For the resonance energy transfer, $(^7/_2{}^*)_a(^5/_2)_b \rightsquigarrow (^7/_2)_a(^7/_2{}^*)_b$, $\delta \simeq 0$ and $\Omega_L \simeq 0.3$ cm. From eq 3 we obtain

$$k_e^\circ = 1.184 \times 10^{12} H^2 \Omega z \quad (5)$$

where $z = 5$ is the number of 1nn and $H = \langle a^*b|\mathcal{H}|ab^*\rangle \simeq 3.4 \times 10^{-4}$ cm^{-1}. Schenk and Guedel[6] assumed that $\mathcal{H}$ is an intercluster exchange operator. Hence, $J_{ab} \simeq H << 0.1$ cm^{-1} and $J_{ab} \geq J_{aa}, J_{bb}$. The use of the intercluster exchange parameters $J_{aa} = 0.6$ cm^{-1} and $J_{bb} = 2.5$ cm^{-1} by Wrobleski et al.[5] in their analysis of the heat capacity data for the chloride salt is therefore incorrect. Intercluster exchange may even be smaller because another mechanism may contribute significantly to k_e°.

Since the $\Delta S = 0$ and $\Delta S = 1$ trimer transitions are allowed by intracluster exchange and single-ion spin–orbit coupling, energy transfer is also possible by a multipole interaction between a and b. We give an estimate of the rate for the case of the dipole–dipole term. The transitions of interest are zero phonon lines so the donor emission probability can be obtained from the oscillator strength of the absorption process. Equation 17 of Dexter[15] is appropriate and in terms of oscillator strengths is

$$k_{a\rightarrow b} = \sum_b {}^9/_{16} f_a f_b c (e^2/mc^2\pi\bar{\nu})^2 (E_0/\kappa^{1/2}n^{1/2}E_c)^4 \Omega_{ab} (\alpha_{ab}{}^2/R_{ab}{}^6) \quad (6)$$

where α_{ab} gives the angular dependence of the transition dipoles, R_{ab} is the separation between the centers of the clusters, f_a and f_b are the oscillator strengths (per cluster) for the transitions $(^7/_2)_a \rightarrow (^7/_2{}^*)_a$ and $(^5/_2)_b \rightarrow (^7/_2{}^*)_b$, respectively, and the remaining quantities are defined elsewhere.[15] The factor α_{ab} is defined as

$$\alpha_{ab} = \sin\theta_a \sin\theta_b \cos\phi - 2\cos\theta_a \cos\theta_b \quad (7)$$

where θ_a and θ_b specify the directions of the transition dipoles with respect to the vector R_{ab} and ϕ is the azimuthal angle between the two dipoles. For the orientationally averaged dipole–dipole interaction, $\alpha_{ab} = {}^2/_3$. The transitions in the 740–780-nm region are predominantly xy-polarized. In the absence of a low-temperature crystal structure, we assume for simplicity x-polarized transition dipoles and ignore corrections for the refractive index and effective electric field. Equation 6 becomes

$$k_{a\rightarrow b} = \sum_b 1.36 \times 10^{32} (f_a f_b \Omega_{ab}/\bar{\nu}^2)(\alpha_{ab}{}^2/R_{ab}{}^6) \quad (8)$$

where R_{ab} is in angstroms and the resonant transitions occur at $\bar{\nu} = 12893$ cm^{-1}. Using $\Omega_{ab} = 0.3$ cm, $f_b = {}^1/_{10} f_a = 24 \times 10^{-9}$, and $R_{ab} = 8.06$–9.14 Å (section 2.1), we obtain $k_e \simeq 1.9 \times 10^4$ s^{-1}. A similar value, $k_e = 1.2 \times 10^4$ s^{-1}, is obtained if we assume $\alpha_{ab} = {}^2/_3$. Inclusion of 2nn clusters will increase k_e, and the reasonable agreement with the experimental value $k_e^\circ \approx 2 \times 10^5$ s^{-1} suggests that the dominant mechanism is a simple dipole–dipole interaction.

Inspection of Figure 2 shows clear evidence for a to b energy transfer. Three specific cases are denoted by arrows. The near-resonance condition is satisfied, and it appears that energy transfer occurs between higher lying excited states; e.g., at 749.5 nm we may have $(^3/_2{}^*)_a(^3/_2)_b \rightsquigarrow (^3/_2)_a(^1/_2{}^*)_{b(1)}$. However, the temperature dependence follows $P_{5/2}$ in all cases. This is clearly indicated at 744.5 nm, where no leakage of the strong $(^1/_2)_a \rightarrow (^1/_2{}^*)_{a(1)}$ transition is detected at low temperatures. In this case a near-resonance energy transfer $(^1/_2{}^*)_{a(1)}(^1/_2)_{b(2)} \rightsquigarrow (^1/_2)_{a(1)}(^1/_2{}^*)_{b(2)}$ should follow $P_{1/2}$. This result shows that energy transfer between higher excited states is quenched by a faster intracluster relaxation process. The observed energy transfer is due to a fast decay (k_x) from $S_a{}^*$ to $(^7/_2{}^*)_a$ followed by the mechanism $(^7/_2{}^*)_a(^5/_2)_b \rightsquigarrow (^7/_2)_a(^7/_2{}^*)_b$. We estimate $k_x \geq 10^7$ s^{-1} from the rise times of the decay curves for the $(^7/_2{}^*)$ emission with excitation at 450 nm.

Registry No. $[Cr_3O(CH_3CO_2)_6(H_2O)_3]Cl$, 35268-73-6.

(14) Denning, R. G.; Ironside, C. N.; Thorne, J. R. G.; Woodwark, D. R. *Mol. Phys.* **1981**, *44*, 209.

(15) Dexter, D. L. *J. Chem. Phys.* **1953**, *21*, 836.